THE JOURNAL OF PHYSICAL CHEMISTRY B

Article

pubs.acs.org/JPCB

Interionic Interactions in Imidazolic Ionic Liquids Probed by Soft X-ray Absorption Spectroscopy

Fabio Rodrigues,*[,†] Douglas Galante,[‡] Gustavo M. do Nascimento,[§] and Paulo S. Santos[†]

[†]Departamento de Química Fundamental, Instituto de Química, Universidade de São Paulo, CP 26.077, CEP 05513-970, São Paulo, SP, Brazil

[‡]Departamento de Astronomia, Instituto de Astronomia, Geofísica e Ciências Atmosféricas, Universidade de São Paulo, São Paulo, SP, Brazil

[§]Departamento de Química, Instituto de Ciências Exatas, Universidade Federal de Minas Gerais, 6627, CEP 31270-901, Belo Horizonte, BH, Brazil

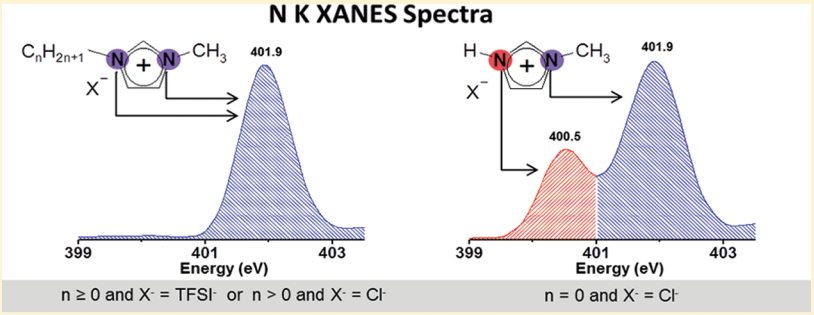

ABSTRACT: This work investigates pure ionic liquids (ILs) derived from an imidazolium ring with different carbonic chains and halides or *bis*(trifluoromethanesulfonilimide) ($TFSI^-$) as anions, using X-ray absorption near edge spectroscopy (XANES) at different energies (N, S, O, F, and Cl edges) to probe the interionic interactions. XANES data show that the interaction with the anion is weaker when the cation is an imidazolium than when the salt is formed by smaller cations, as lithium, independently of the length of the carbonic chain attached to the imidazolium cation. The results also show that, for all studied ILs, it is not observed any influence of the anion on the XANES spectra of the cation, nor the opposite. 1-Methylimidazolium with Cl^-, a small and strongly coordinating anion, presents in the N K XANES spectrum a splitting of the band corresponding to nitrogen in the imidazolic ring, indicating two different chemical environments. For this cation with $TFSI^-$, on the contrary, this splitting was not observed, showing that the anion has a weaker interaction with the imidazolic ring, even without a lateral carbonic chain.

INTRODUCTION

Ionic liquids (ILs) are a family of salts that are liquids at low temperatures (typically under 100 °C, being many of them liquid at room temperature), normally composed of a bulky asymmetric cation and a weakly coordinating anion. Many different combinations of cations and anions could form ionic liquids (some authors[1] estimate about 10^{18} different combinations), but the ionic liquids derived from the imidazolic ring are the most studied ones.[2,3] Parameters like the length of the carbonic chain bonded to the cation or the anion type can drastically change the properties of the ILs, thus being possible to design an ILs for specific applications.[4,5] In most cases, ILs have high thermal stability, a broad electrochemical window, an organized structure at medium distances (in opposition to molecular liquids, that are organized only at small distances) and very low vapor pressure, properties that make them important in many areas like green chemistry, organic and inorganic synthesis, and many others.[6]

The possibility of new applications for these systems in many different areas, with better performance in comparison to molecular liquids, increased the number of scientific studies involving the properties[7] of existing ILs and the search for new ones. Due to the enormous number of possible combinations, the theoretical understanding and modeling of such parameters are very important for a rational choice of the best IL for each application, and the study, at a molecular level,[8] of ILs and the processes in which they are involved becomes mandatory.[9] Although there are many studies involving basic properties of ILs, important details of their structure and interactions are still not completely understood, due, in part, to the complexity of these systems.[10] The presence of ions, polar regions, and apolar chains make ILs a very inhomogeneous medium,[11,12] an inhomogeneity that becomes enhanced in mixtures with water or organic solvents.[13−15] This topic, however, is still very controversial and more studies are necessary to the better knowledge of the structure of these systems.

A very important challenge concerning ionic liquids is to understand the different interactions comprehending both

Received: August 22, 2011
Revised: November 25, 2011
Published: January 6, 2012

interionic, like Coulombic forces, and intermolecular interactions, like hydrogen bonds and van der Waals forces, which, in most cases, cannot be easily distinguished from each other.[16]

To answer the fundamental question of why ionic liquids are liquid, Krossing et al.[17] used an approach based on lattice and solvation energies and quantum chemical calculations to conclude that the liquid state is due to the small lattice enthalpies and large entropy caused by the large size and high flexibility of the ions.[17] In addition, Katoh observed[18] the same UV−vis spectra for two imidazolic ILs, independent of the type of anion (hexafluorophosphate and *bis*(trifluoromethanesulfonylimide)) or whether the IL is pure or in acetonitrile solution. The author concluded that the electronic states of imidazolium cation are not changed by interionic interactions and that the spectra are the simple sum of those from cation and anion. Ando, Siqueira, and co-workers have described the immediate melting of 1-butyl-3-methylimidazolium bromide, an ionic liquid solid at room temperature (melting point around 45 °C), with the addition of sulfur dioxide, and concluded, using molecular dynamics calculations and Raman spectroscopy, that the cation−anion distances remain unchanged. It was proposed that the SO_2 causes the shielding of anion charges and reduces the lattice energy, instead of separating ions.[19,20]

Many techniques have been used to characterize cation−anion interaction in ILs, such as computer simulations,[21] absorption or fluorescence spectroscopy,[22,23] vibrational spectroscopy (pure and with probes),[24−26] and several techniques involving X-rays as, for example, wide-angle X-ray scattering,[27] X-ray photoemission,[28] and X-ray photoelectric spectroscopy,[29] most of them focusing on both interionic and intermolecular interactions at the same time. In this work, the X-ray absorption near edge spectroscopy (XANES) using soft X-rays (200−2500 eV) was employed in the investigation of the interactions observed in the imidazolic ILs, probing the absorption edge of different atoms present in ILs.

The XANES technique promotes the excitation of core electrons. It is an excellent technique to distinguish atoms in nonequivalent chemical neighborhoods, making possible the investigation of molecular structures, types of interactions, and oxidation states around the absorber atom.[30] Each absorption edge is related to a specific atom present in the material, and, more specifically, to a transition that excites a particular atomic core-orbital electron to a free level or to the continuum (ionization of the core orbital) above the Fermi energy. The energies of the edges (or ionization energies) are unique to the type of atom, and hence are signatures of the atomic species present in a material.[31]

In processes with energy close to the edge of the absorption, the de Broglie wavelength of the photoelectron emitted is higher than the atomic distances; thus, the mean free path of the photoelectron is sufficient to cause multiple scatterings.[30,31] This phenomenon turns the XANES spectra sensible to the electronic density around the absorbing atom, implying that it can be used to monitor the oxidation state and changes of unoccupied electronic states due to the chemical environment.[30,31] On the other hand, this technique has low sensitivity to intermolecular forces, like hydrogen bonds and dipole interactions, which makes it of particular importance to isolate interionic from intermolecular effects.

In fact, XANES spectra of "soft" matter ($Z < 18$) are very complex, particularly for molecules with high electronic delocalization, since many pre-edge peaks appear, which can be associated to resonance and/or conjugation effects.[32−34]

The N K-edge XANES spectroscopy has been successfully employed by our group in the study of oxidation states and interactions in aromatic and/or conjugated systems where the study of many model compounds assists the interpretation of the spectra of more complex materials, such as polymers and ionic liquids.[35−38] It was demonstrated,[36] for the first time, the viability to perform N K-edge XANES measurements in solutions using ILs, as solvents, being possible to study the interactions between solute and solvent molecules. For instance, for potassium 2,4-dinitrophenolate, the interaction with the 1-butyl-3-methylimidazolium tetrafluoroborate causes the splitting of the $-NO_2$ band, and it was possible to observe the conversion of polyaniline in its insulating state (emeraldine base) to its conducting state (emeraldine salt), after dissolution in 1-ethyl-3-methylimidazolium ethylsulfate.[35]

In this work, we have used the XANES technique to probe the electronic environment around different atoms that compose both the cation and anion of different imidazolic ionic liquids, emphasizing those with chloride and *bis*(trifluoromethanesulfonylimide) anions, due to the drastically different properties of these ions. Because of the low sensitivity of this technique to most intermolecular interactions, the differences observed here can be attributed to Coulombic forces, helping to isolate these effects in ILs.

EXPERIMENTAL SECTION

a. Materials. 1-Chlorobutane, 1-bromoetane, 1-bromobutane, 1-bromohexane, 1-bromooctane, 1-methylimidazole, 1,2-dimethylimidazole, 1-methylimidazolium chloride ([1-MIm]Cl), and lithium *bis*(trifluoromethanesulfonyl)imide (LiTFSI) were purchased from Aldrich. All bromoalkanes and chloroalkanes were distillated when received and stored under refrigeration. 1-Methylimidazole and 1,2-dimethylimidazole were distilled under vacuum and stored under nitrogen and refrigeration for a maximum of 2 weeks before being used. The salts [1-MIm]Cl and LiTFSI were used as received.

b. Synthesis of Ionic Liquids. The methodology to synthesize, purify, and characterize ILs was adapted from the literature[39] and described elsewhere[26] and will be briefly reported here.

The synthesis of ILs with chloride or bromide anions (see Figure 1) consists basically of reacting 1-methylimidazole or 1,2-dimethylimidazole with 1-haloalkane (1:1.1 molar ratio) under nitrogen atmosphere in a silicone oil bath ($T \approx 70$ °C) and vigorous stirring for at least 6 h. After the reaction completion, the product was purified in order to remove the unreacted material. ILs that are solid at room temperature were purified by recrystallization with ethyl acetate or tetrahydrofurane (about half of the IL volume is necessary), while those that are liquid at room temperature were purified by successive extractions with ethyl acetate or tethahydrofurane. At last, purified ILs were dissolved in dichloromethane and dried by the addition of anhydrous $MgSO_4$. The dichloromethane was evaporated and recuperated, and the dry ILs were sealed and stored in a desiccator, under vacuum.

For the synthesis of ILs with $TFSI^-$ anion, it was proceeded by an anion exchange, adding a concentrated aqueous solution of LiTFSI into a solution containing IL with Br^- anion (1:1.1 molar ratio between IL and LiTFSI). The resulting IL with $TFSI^-$ anion (hydrophobic) was separated, and afterward, the IL was washed with water and dried again. The same

dx.doi.org/10.1021/jp208094p | J. Phys. Chem. B 2012, 116, 1491−1498

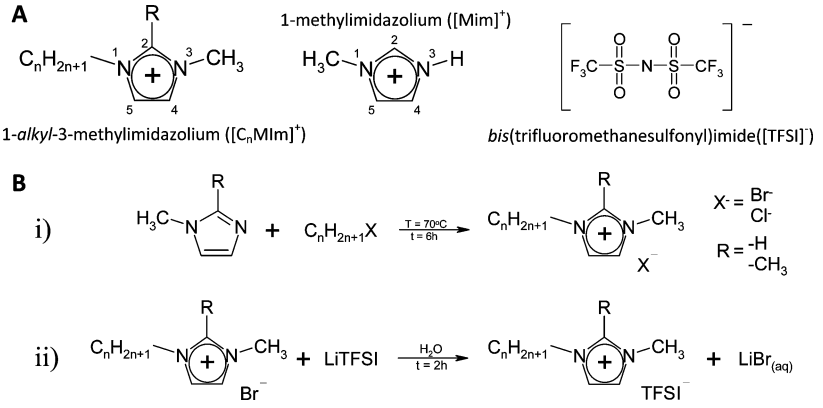

Figure 1. Schematic representation of (A) some ions used in the experiments—for the cations, the number of the atoms in the ring is shown; (B) (i) synthesis of halogenated imidazolium ionic liquids and (ii) anion exchange to obtain ILs with $TFSI^-$ anion. In the text, the nitrogen atoms numbered as 1 and 3 will be named N1 and N3, respectively.

procedure was used to synthesize 1-methylimidazolium *bis*(trifluoromethanesulfonyl)imide ([1-MIm]TFSI), using [1-MIm]Cl and LiTFSI.

Some of the products have been analyzed by NMR and compared with the literature,[39] as well as by MALDI-ToF and Raman and infrared spectroscopy, and no signal of impurity was detected. The XANES spectra were in accordance with those obtained for some commercial high-purity ILs, so any impurity, if present, is not interfering in the measurements.

In this work, imidazolic ILs will be abbreviated as $[C_nMIm]^+$ for 1-*alkyl*-3-methylimidazolium and $[C_nMMIm]^+$ for 1-*alkyl*-2,3-dimethylimidazolium, where *n* is the number of carbons in the alkyl chain.

c. XANES Measurements. Nitrogen, oxygen, and fluor K-edge XANES spectra were obtained at the spherical grating monochromator (SGM) beamline (dipole magnetic field of 1.65 T and critical energy of 2.08 keV) at the Brazilian National Synchrotron Light Laboratory, LNLS (electron energy of the storage ring is 1.37 GeV). The SGM beamline (The spectral resolution $E/\Delta E$ is better than 3000. 3000 is the right value to SGM beamline. The other value, 5000, is to SXS beamline, which is different.) has a focused beam of, roughly, 0.5 mm^2 spot size, and the spectra were recorded in total electron yield (TEY) detection mode, with the sample compartment pressure at 10^{-8} mbar. Measurements were done with the sample surface normal to the beam. All energy values observed in the N, O, and F K-edge spectra were calibrated using the first resonant peak at 405.5 eV in N K-edge XANES spectra for potassium nitrate.[40]

Sulfur K-edge XANES spectra were collected on the soft X-ray spectroscopy (SXS) beamline (LNLS, Brazil) equipped with a double Si crystal monochromator with toroidal focusing mirror with a focused beam of 2.0 × 3.0 mm^2 spot size (the spectral resolution $E/\Delta E$ of the SXS beamline is better than 5000). Spectra were recorded in total electron yield detection mode and with the sample chamber at ca. 10^{-8} mbar. All energy values in the S K-edge spectra were calibrated using the band at 2520.2 eV, referent to the L_{III} $2p_{3/2}$ edge of metallic molybdenum.[41]

Chlorine L-edge XANES spectra were collected on the toroidal grating monochromator (TGM) beamline, with the spectral resolution $E/\Delta E$ of toroidal grating better than 530 and a focused beam of, roughly, 2 × 0.5 mm^2 spot size. The spectra were recorded in total electron yield (TEY) detection mode, with the sample compartment pressure at 10^{-8} mbar. Measurements were done with the sample surface normal to the beam.

The samples were fixed in a sample holder made of aluminum or stainless steel, placed perpendicular to the beam axis. The solid samples were fixed with copper-made, electron-microscopy adhesive tape placed directly over the surface of the sample holder, while the liquid samples were deposited in cylindrical wells with 5 mm diameter. As dry ILs are very viscous, they did not drain. A polarization ring was disposed in front of the sample holder with an electrical potential of about +100 V to avoid charging effects, and each sample was duplicated and measured three times, the results showing an invariance of the spectra for all the measurements.

The cautions necessary to work with liquid samples and its sample holder have been described elsewhere.[36] The solid samples were fixed in a copper double-faced adhesive tape, which shows a signal in the O K-edge. Hence, the spectra in the O K-edge region are shown with the respective spectrum for the copper tape, in order to identify the different contributions. Some spectra had their baseline subtracted, for a better visualization.

RESULTS AND DISCUSSION

Figure 2 displays the N K-edge XANES spectra of 1-butyl-3-methylimidazolium ($[C_4MIm]^+$) with different anions ($[Cl]^-$, $[Br]^-$, $[PF_6]^-$, $[TFSI]^-$). The spectra show a very similar spectral profile, being dominated by a strong band at 401.9 eV that was assigned to the 1s → 2pπ^* transition of the nitrogen of the imidazolium ring. The other bands observed at 408.5 and 414.8 eV can be associated to 1s → σ^* transitions of the nitrogen in the imidazolium ring.[36]

It is known that the neutral imidazole molecule presents a X-ray spectrum at the N K-edge very different from those observed in ILs.[42] In particular, two different main peaks attributed to N1 and N3 can be observed (see Figure 1 for the number of each atom in the ring) in the region between 400.0 and 402.0 eV, while for ILs there is the presence of just one major peak, which indicates the equivalence between the two nitrogen atoms.

A small difference between the spectra can be observed in the shoulder at ca. 405.5 eV (see Figure 2), which is probably related to a long distance organization of the salts, since this shoulder is more pronounced in those ILs that are solid at room temperature ($[C_4MIm][Cl]$ and $[C_4MIm][Br]$). It can be noticed that, in the spectrum in Figure 2D, corresponding to $[C_4MIm][TFSI]$, a band in this region can also be observed,

dx.doi.org/10.1021/jp208094p | J. Phys. Chem. B 2012, 116, 1491–1498

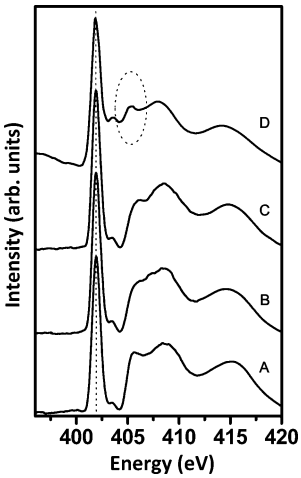

Figure 2. N K XANES spectra of IL $[C_4MIm]^+$ with different anions: (A) Cl^-, (B) Br^-, (C) PF_6^-, and (D) $TFSI^-$. The dashed region in spectrum D corresponds to the contribution of the strongest peak for TFSI anion.

but it can be assigned to the nitrogen in the cation, as will be discussed later. Hence, with the exception of this shoulder, the energy values for the transitions do not change and the similarity between the spectra strongly suggests that the nature of the anion has a small influence on the electronic structure surrounding the nitrogen of the imidazolium ring. This result is in good accordance with the literature, especially with the results obtained by Katoh,[18] which shows that the electronic absorption spectra of the cation remains the same when the anion is changed.

Figure 3 shows the N K XANES spectra of $[C_nMIm][Br]$ with different carbonic chains (n = 2, 4, 6, and 8), and in the

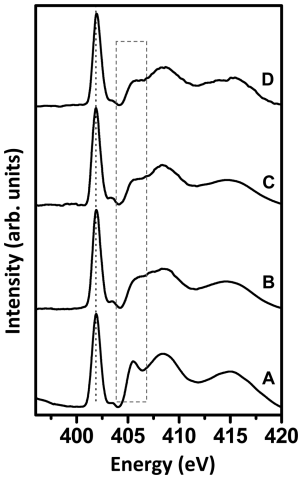

Figure 3. N K XANES spectra of $[C_nMIm]Br$ with different carbonic chains: (A) ethyl (n = 2), (B) butyl (n = 4), (C) hexyl (n = 6), and (D) octyl (n = 8).

same way, as verified in Figure 2, the spectra are almost the same for all imidazolic ionic liquids. The spectra of $[C_2MIm][Br]$ (Figure 3A) have the most pronounced shoulder at ca. 405.5 eV, and in sequence, $[C_4MIm][Br]$ (Figure 3B) has the second one. Since the increasing of carbonic chain length decreases the melting point, up to 8 carbons, these two are solid at room temperature and $[C_6MIm][Br]$ and $[C_8MIm][Br]$ (Figure 3B and C) are liquid at room temperature, which corroborates the conclusion from Figure 2, that this shoulder could be related to the crystalline structure of the IL in solid state. New studies aiming to a more detailed attribution are now in progress in our group.

According to Krossing et al.,[17] in the solid state, the ILs have higher lattice energy and the anions change the electronic distribution around the nitrogen of the cation. Our results show that this change has no influence on the main peak observed in the N K-edge spectra for ILs. However, a small modification in the relative intensity and the line shape of the peak near 405.5 eV is seen, suggesting that, although the interaction with anions increases in the solid state, it remains weak, as expected from the low melting points of these samples when compared with other classes of salts.

The results shown above concern the influence of both anion nature and carbonic chain length in the electronic neighborhood of the nitrogen atom in the anion. It can be seen that there are no significant alterations on the spectra of pure ILs (Figures 2 and 3) with carbon chains of different lengths ($n \geq 2$) and with different anions, indicating a similar charge distribution around N1 and N3. This result is in accordance with those shown by Urahata and Ribeiro,[21] that found very similar partial charge and Lennard-Jones parameters for N1 and N3 atoms in several cations $[C_nMIm]^+$ (n = 1, 2, 4, and 8), independent of the anion, which suggests that for $n \geq 1$ the carbonic chain can play a major role, masking the anion effect on electronic distribution. The similar XANES spectra observed for very different anions such as $[Cl]^-$ (Figure 2A) and $TFSI^-$ (Figure 2D) corroborate this conclusion.

A question that still remains is the limit of the influence of the carbon chain length on the electronic distribution around the imidazolium cation, since in the cases discussed before different carbonic chains and anions have been analyzed together. In order to separate the influence of each parameter (anion type and carbon chain length), we obtained the XANES spectra for some salts without carbon chains bonded to the nitrogen atoms in the imidazolium ring. Figure 4 shows the spectra of

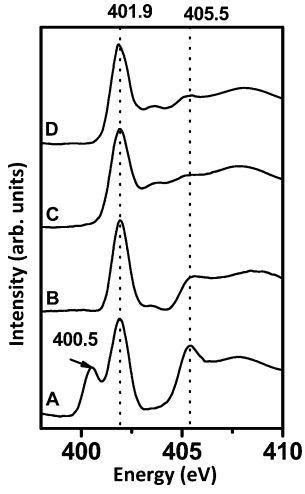

Figure 4. N K-edge XANES spectra for (A) [1-Mim]Cl, (B) $[C_4MIm]Cl$, (C) [1-Mim]TFSI, and (D) $[C_4MIm]TFSI$.

1-methylimidazolium chloride ([1-MIm][Cl], Figure 4A) and 1-methylimidazolium *bis*(trifluoromethanesulfonyl)imide ([1-MIm][TFSI], Figure 4C), which are imidazolic salts without a lateral

dx.doi.org/10.1021/jp208094p | J. Phys. Chem. B 2012, 116, 1491–1498

carbon chain ($n = 0$). For comparison, the N K-XANES spectra of [C_4Mim][Br] (Figure 4B) and [C_4Mim][TFSI] (Figure 4D) are also displayed.

Comparing the spectra in Figure 4A and B, one can observe the splitting of the principal peak at 401.9 eV that is assigned to the 1s → 2pπ^* transition on the N K XANES spectra of [1-MIm][Cl] (Figure 4A). The peak at 401.9 eV remains in the spectra, but now a new peak at lower energy (400.5 eV) appears, a different behavior from those observed for ILs (see Figure 2 and 3). Since [1-Mim][Cl] and [C_4MIm][Cl] have the same anion, we can suppose that the signal at 401.9 eV is due to N3 (the one with a methyl group, as can be seen in Figures 2 and 3), while that new peak at 400.5 eV is more probably due to N1 (the one with −H).

This result can be understood according to the behavior of ILs demonstrated by Urahata and Ribeiro[21] to ILs with different carbonic chains, using molecular dynamics. The increase in the chain length increases the number of possible configurations of the chain, resulting in a more effective steric effect. The $[1\text{-MIm}]^+$ cation, without carbonic chain (Figure 4A), allows the $[Cl]^-$ anion to be closer from N3, which does not happen in N1, with the methyl group.

On the other hand, the −H group at $[1\text{-MIm}]^+$ is extremely acidic and interacts strongly with $[Cl]^-$, a small and highly coordinating anion, letting the anion far from N3. The hydrogen bond around N1 changes the electronic density, shifting the band to 400.5 eV (Figure 4A). The same behavior is not observed for any IL ($n > 0$), where the steric effect and the absence of an acid hydrogen bonded to the nitrogen contribute to move the anion away from the neighborhood of the nitrogen atoms. In this case (Figure 4B−D), the electronic densities around N1 and N3 are comparable and just one band is observed in the XANES spectra.

This is an important result, since it shows, for the first time, the electronic distribution around the nitrogen in the imidazolium cation being affected by the anion. In a first interpretation, it can be considered as a possible explanation the fact that the nitrogen without carbon chain has intrinsically a different charge distribution when compared to that with the chain, due to the inductive effect of the methyl group, which can lead to a different XANES spectrum. Analyzing Figure 4C, however, it can be observed that the same cation has a different XANES spectrum with $[TFSI]^-$ anion, again presenting just the peak at 401.9 eV, as observed for ILs, with $n > 0$. Although the cation has now a very concentrated charge around N3, at this time, the anion has a much more delocalized charge and is weakly coordinating, thus not contributing to a strong electrostatic interaction. Theoretical calculations for these systems are available in the literature, as can be seen in the Supporting Information part of the work by Thompson and co-workers.[43]

Hence, it is clear that the new band at 400.5 eV is due to the interaction between chloride and N1 atom of imidazolium in [1-MIm][Cl].

These results lead to the conclusion that, to have major effects caused by electrostatic interactions, it is necessary that both the cation and anion contribute to the process. This is observed for [1-MIm][Cl]. When the system is composed of a highly coordinating anion and a bulky asymmetric cation with delocalized charge, like [C_4MIm][Cl], or by a cation with concentrated charge but a weakly coordinating anion, with delocalized charge, like [1-MIm][TFSI], the Coulombic interaction remains very weak and the interionic interactions are dominated by intermolecular forces. In the extreme case of a very large cation with delocalized charge and with a weakly coordinating anion, like [C_4MIm][TFSI], the Coulombic forces are even weaker and intermolecular forces play a much more important role.

For ILs, the magnitude of the interionic forces, however, has no direct correlation with their physical state, since several intermolecular forces are also acting, many times in a stronger way. Three of the compounds, [1-MIm][Cl], [1-MIm][TFSI], and [C_4MIm][Cl], are solid at room temperature and just [C_4MIm][TFSI] is liquid, but among these, only [1-MIm][Cl] shows the splitting in the N K XANES spectrum being the salt with the highest melting point.

After analyzing the imidazolium cation in different conditions, it is important to understand the changes in the electronic structure of the anion. In this work, special attention will be given to $[Cl]^-$ and $[TFSI]^-$. Figure 5 shows the Cl L_{II} ($2p_{1/2}$)-edge[41] XANES spectra of $[Cl]^-$ in [1-MIm]Cl

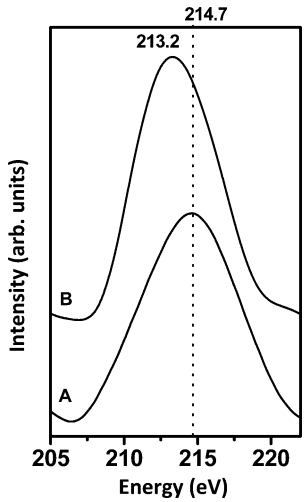

Figure 5. Cl L_{II} ($2p_{1/2}$)-edge XANES of (A) [1-MIm]Cl and (B) [C_4MIm]Cl. The spectra have been manipulated with smoothing and baseline correction for a better visualization, preserving the original shape and frequency.

(Figure 5A) and [C_4MIm]Cl (Figure 5B), in which a shift of about 1.5 eV can be observed, corroborating the data obtained in Figure 4 and the conclusion that a differential interaction between chloride and the two cations is occurring. The difference between $[1\text{-MIm}]^+$ and $[C_4MIm]^+$ is the carbon chain length that separates the ions.

The same result is not expected for $TFSI^-$, since it has been observed that [1-MIm][TFSI] and [C_nMIm][TFSI] ($n > 1$) have almost the same spectra. LiTFSI, a precursor in the synthesis of ILs with $[TFSI]^-$ (see the Experimental Section), was used as a standard to compare the effects of different cations on the spectra of $[TFSI]^-$. Unlike the imidazolium cation, Li^+ is a very small cation with a high charge concentration, resulting in a stronger interaction with the anion. In order to analyze the effect of different cations on the electronic structure of $[TFSI]^-$, the K-edge XANES spectra of different elements were measured in order to probe the anion structure.

Figure 6 shows N K XANES spectra of different imidazolic salts having $[TFSI]^-$ as the anion (Figure 6B−E), with R = −H or $-CH_3$ and $n = 0$, 4, and 6 and with Li^+ cation (Figure 6A). It is possible to see a coincidence in energy (around 402 and 405 eV) between the bands attributed to the nitrogen from

dx.doi.org/10.1021/jp208094p | J. Phys. Chem. B 2012, 116, 1491−1498

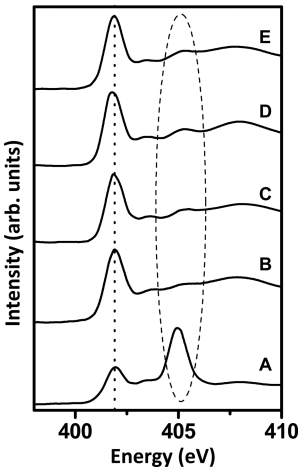

Figure 6. N K XANES spectra of different ILs with TFSI anion: (A) LiTFSI (standard), (B) [1-MIm]TFSI, (C) [C_4MIm]TFSI, (D) [C_6MIm]TFSI, and (E) [C_4MMIm]TFSI. The circled region shows the shoulder at ca. 405.0 eV attributed to nitrogen on anion.

$[TFSI]^-$ (Figure 6A) and from the cation (Figure 6B–E), as previously pointed out (see Figure 2). This coincidence makes the study of nitrogen of the anion a very difficult task by this technique. The shoulder observed at 405 eV in [C_nMIm]-[TFSI] ionic liquids, as emphasized in Figure 2, is attributed to the signal from the anion and not from the cation.

The data presented previously show that the N K XANES spectra are similar for all ILs, independent of the anion and carbon chain length. This fact can also be observed in spectra B and F of Figure 6, showing that the addition of a methyl group in carbon 2, responsible for significant changes in the intermolecular interactions,[44] has a nonmeasurable influence on the electronic structure around the nitrogen atom, by N K-XANES.

Figure 7 shows the XANES spectra at the sulfur K-edge. It can be seen that the ILs have similar spectra (see Figure 7B–E),

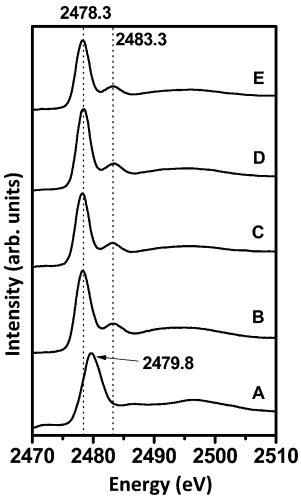

Figure 7. S K XANES of (A) LiTFSI, (B) [1-MIm]TFSI, (C) [C_4MIm]TFSI, (D) [C_6MIm]TFSI, and (E) [C_4MMIm]TFSI.

with the band at 2478.3 eV being attributed to the Kα_1 transition of sulfur atoms.[45] The S K-edge XANES spectrum of LiTFSI displays an upshift of about 1.5 eV in comparison to the spectra of ILs. Probably, the formation of ion associations and the concentration of negative charge in the nitrogen atom lead to the energy upshift of the unoccupied states in the sulfur atoms.

Another marked difference is the existence of a secondary peak (2483.4 eV) in the spectra corresponding to ILs (Figure 7B–E), which is not seen in the LiTFSI spectrum. This secondary peak can be attributed to the presence of a different chemical environment around the sulfur atoms, caused by the highly delocalized charge in the anion and by the mobility of ions in the ILs, causing a shift in the spectra depending on the relative position and conformation of cation and anion. These results are in accordance with the literature that proposes different conformers with different energies of $[TFSI]^-$ in imidazolic ILs.[46,47] On the other hand, the LiTFSI salt is a highly organized system and Li^+ is a very small ion with concentrated charge that strongly interacts with the anion (around the nitrogen), which results in just one band, due to the unique arrangement.[48]

The behavior described for the sulfur in the $[TFSI]^-$ indicates that the interaction with the anion is much less intense for imidazolium cations, independent of the substituent, including $[1\text{-MIm}]^+$, than for lithium cations. It leads to the conclusion that the separation between cation and anion occurs not just because of the carbon chain but mainly because of the large size of both the cation and anion.

The same behavior observed for sulfur atoms is also observed for oxygen and fluorine atoms in $[TFSI]^-$: the spectra for all the imidazolium salts are very similar, including those corresponding to [1-MIm][TFSI], while a shift to higher energy is observed only for the LiTFSI salt. Figure 8 displays the O and F K-edge XANES spectra for some samples, [C_4MIm][TFSI] and

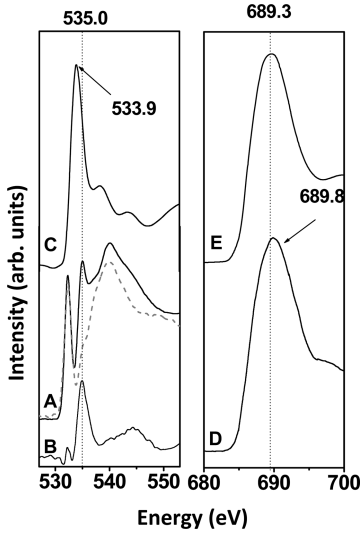

Figure 8. (A) O K XANES of the salts LiTFSI (the gray line in IA represents the spectrum from adhesive from copper tape where the LiTFSI was fixed, and the spectrum in black represents the sum of LiTFSI plus adhesive); (B) O K XANES of LiTFSI (subtracted the contribution from copper tape); (C) O K XANES of the salts [C_4MIm]TFSI; (D) F K XANES of the salts LiTFSI; and (E) F K XANES of the salts [C_4MIm]TFSI.

LiTFSI, since the spectra for all ILs are essentially identical, as observed for S and N edges.

It can be seen in the spectra around the fluorine K-edge (Figure 8, right panel) that the band shape is exactly the same

dx.doi.org/10.1021/jp208094p | J. Phys. Chem. B 2012, 116, 1491–1498

for imidazolium and lithium samples, in opposition to what was observed at the S K-edge (Figure 7), in which different peaks could be observed. In addition, the shift in the band is 0.5 eV, smaller than those observed in the sulfur edge, indicating that Li^+ causes smaller changes in the electronic structure around fluorine than around sulfur, which can be explained by the fact that Li^+ interacts with the center of the molecule, which is closer to sulfur. Another remarkable fact is the presence of a single broad band indicating that all six fluorine atoms in the analyzed samples are in similar chemical environments, for imidazolium and lithium salts.

The shift observed for the O K-edge (Figure 8, left panel) for LiTFSI (Figure 8B) and $[C_4MIm][TFSI]$ (Figure 8C) is of ca. 1.1 eV, an intermediary value when compared to fluorine and sulfur. The comparison of the band shape, however, is not very accurate, since there is an interference for solid samples caused by the oxygen spectra of the adhesive (gray line in Figure 8A) in the copper tape used to fix the samples (see the Experimental Section). The subtraction of the signal of the copper tape, however, has been proceeded (Figure 8B). This signal was subtracted to calculate the maximum of the LiTFSI band.

CONCLUSION

For the first time, soft X-ray absorption spectroscopy around the edges of different elements was used in the investigation of both cations and anions of imidazolic ionic liquids. By changing the edge, it was possible to monitor both imidazolium cations (with different structures) and anions that form these systems.

It is known that the Coulombic interaction between cation and anion in ILs is very weak, which is the main reason for their low melting point, and that intermolecular forces dominate in these systems. The presented systematic XANES study of different elements indicates that the presence of a carbon chain in both nitrogen atoms of the imidazolium cation reduces the Coulombic interaction, for any chain length. The anion properties were shown to produce minor effects on the interactions, in these cases.

Just in the case of the absence of a carbon chain in one of the nitrogens of the imidazolic salt, the differential effect of the anions was observed, which leads to the conclusion that both a long carbon chain in the cation and the presence of a low coordinating anion, separately or in combination, cause the low electrostatic interaction in ILs.

XANES data also show that the interaction with the anion is much less intense when the cation is an imidazolium than when the salt is formed by a lithium cation, independent of the length of carbon chain bonded in the imidazolium cation. On the other hand, the lithium cation, much smaller than $[C_nMIm]^+$, forms an ion association with the $[TFSI]^-$ anion, and changes in the K-XANES spectra are observed for the probed atoms. These changes are more intense in the central region of the molecule, near the nitrogen, and weaker in the extremities, around fluorine atoms.

In agreement with previous results in the literature, the data shown here can be clearly interpreted as being due to the weak electrostatic interaction between cation and anion in room temperature ionic liquids, where the spectrum is the simple sum of the contributions from cations and anions.[18] Thus, it is possible to infer the major importance of intermolecular forces in the structure of ionic liquids, as compared to the Coulombic forces.

AUTHOR INFORMATION

Corresponding Author

*E-mail: farod@iq.usp.br.

ACKNOWLEDGMENTS

This work has been supported by FAPESP, CNPq, and CAPES (Brazilian agencies) through fellowships and financial support. The authors would like to thank the LNLS for the use of the TGM beamline (Proposal Nos. 5832 and 9894), SGM beamline (Proposal Nos. 7799 and 9281), and SXS beamline (Proposal Nos. 7809 and 9354).

REFERENCES

(1) Holbrey, J. D.; Seddon, K. R. *Clean Technol. Environ. Policy* **1999**, *1*, 223−226.
(2) Dupont, J. *J. Braz. Chem. Soc.* **2004**, *15*, 341−350.
(3) Dupont, J.; Suarez, P. A. Z. *Phys. Chem. Chem. Phys.* **2006**, *8*, 2441−2452.
(4) Davis, J. R. Jr. *Chem. Lett.* **2004**, *33*, 1072−1077.
(5) Larsen, A. S.; Holbrey, J. D.; Tham, F. S.; Reed, C. A. *J. Am. Chem. Soc.* **2000**, *122*, 7264−7272.
(6) Welton, T. *Chem. Rev.* **1999**, *99*, 2071−2083.
(7) El Seoud, O. A.; Koschella, A.; Fidale, L. C.; Dorn, S.; Heinze, T. *Biomacromolecules* **2007**, *8*, 2629−2647.
(8) Arantes, G. M.; Ribeiro, M. C. C. *J. Chem. Phys.* **2008**, *128*, 114503.
(9) Weingärtner, H. *Angew. Chem., Int. Ed.* **2008**, *47*, 654−670.
(10) Padua, A. A. H.; Gomes, M. F.; Lopes, J. *Acc. Chem. Res.* **2007**, *40*, 1087−1096.
(11) Singh, T.; Kumar, A. *J. Phys. Chem. B* **2007**, *111*, 7843−7851.
(12) Lopes, J. N. A. C.; Padua, A. A. H. *J. Phys. Chem. B* **2006**, *110*, 3330−3335.
(13) Fazio, B.; Triolo, A.; Di Marco, G. *J. Raman Spectrosc.* **2008**, *39*, 233−237.
(14) Anderson, J. L.; Ding, J.; Welton, T.; Armstrong, D. W. *J. Am. Chem. Soc.* **2002**, *124*, 14247−14254.
(15) Li, W.; Zhang, Z.; Han, B.; Hu, S.; Xie, Y.; Yang, G. *J. Phys. Chem. B* **2007**, *111*, 6452−6456.
(16) Fujisawa, T.; Nishikawa, K.; Shirota, H. *J. Chem. Phys.* **2009**, *131*, 244519.
(17) Krossing, I.; Slattery, J. M.; Daguenet, C.; Dyson, P. J.; Oleinikova, A.; Weingärtner, H. *J. Am. Chem. Soc.* **2006**, *128*, 13427−13434.
(18) Katoh, R. *Chem. Lett.* **2007**, *36*, 1256−1257.
(19) Ando, R. A.; Siqueira, L. J. A.; Bazito, F. C.; Torresi, R. M.; Santos, P. S. *J. Phys. Chem. B* **2007**, *111*, 8717−8719.
(20) Siqueira, L. J. A.; Ando, R. A.; Bazito, F. C.; Torresi, R. M.; Santos, P. S.; Ribeiro, M. C. C. *J. Phys. Chem. B* **2008**, *112*, 6430−6435.
(21) Urahata, S. M.; Ribeiro, M. C. C. *J. Chem. Phys.* **2004**, *120*, 1885−1863.
(22) Paul, A.; Samanta, A. *J. Chem. Sci.* **2006**, *118*, 335−340.
(23) Coleman, S.; Byrne, R.; Minkovska, S.; Diamond, D. *J. Phys. Chem. B* **2009**, *113*, 15589−15596.
(24) Jeon, Y.; Sung, J.; Seo, C.; Lim, H.; Cheong, H.; Kang, M.; Moon, B.; Ouchi, Y.; Kim, D. *J. Phys. Chem. B* **2008**, *112*, 4735−4740.
(25) Fujisawa, T.; Fukuda, M.; Terazima, M.; Kimura, Y. *J. Phys. Chem. A* **2006**, 6164−6172.
(26) Rodrigues, F.; Santos, P. S. *Vib. Spectrosc.* **2010**, *54*, 123−126.
(27) Katayanagi, H.; Hayashi, S.; Hamaguchi, H.; Nishikawa, K. *Chem. Phys. Lett.* **2004**, *392*, 460−464.
(28) Kanai, K.; Nishi, T.; Iwahashi, T.; Ouchi, Y.; Seki, K.; Harada, Y.; Shin, S. *J. Electron Spectrosc. Relat. Phenom.* **2009**, *174*, 110−115.
(29) Caporali, S.; Bardi, U.; Lavacchi, A. *J. Electron Spectrosc. Relat. Phenom.* **2006**, *151*, 4−8.
(30) Durham, P. J. In *X-ray Absorption*; Koningsberger, D. C., Prins, R., Eds.; John Wiley & Sons: New York, 1988; pp 53−84.

(31) Rehr, J. J.; Albers, R. C. *Rev. Mod. Phys.* **2000**, *72*, 621−654.
(32) Hennig, C.; Hallmeier, K. H.; Bach, A.; Bender, S.; Franke, R.; Hormes, J.; Szargan, R. *Spectrochim. Acta, Part A* **1996**, *52*, 1079−1083.
(33) Hennig, C.; Hallmeier, K. H.; Szargan, R. *Synth. Met.* **1998**, *92*, 161−166.
(34) Francis, J. T.; Hitchcock, A. P. *J. Phys. Chem.* **1992**, *96*, 6598−6610.
(35) Rodrigues, F.; Do Nascimento, G. M.; Santos, P. S. *Macromol. Rapid Commun.* **2007**, *28*, 666−669.
(36) Rodrigues, F.; Do Nascimento, G. M.; Santos, P. S. *J. Electron Spectrosc. Relat. Phenom.* **2007**, *155*, 148−154.
(37) Do Nascimento, G. M.; Temperini, M. L. A. *Quim. Nova* **2006**, *29*, 823−828.
(38) Do Nascimento, G. M.; Constantino, V. R. L.; Landers, R.; Temperini, M. L. A. *Macromolecules* **2004**, *37*, 9373−9385.
(39) Huddleston, J. G.; Visser, A. E.; Reichert, M.; Willauer, H. D.; Broker, G. A.; Rogers, R. D. *Green Chem.* **2001**, *3*, 156−164.
(40) Vinogradov, A. S.; Akimov, V. N. *Opt. Spectrosc.* **1998**, *85*, 53−59.
(41) Thompson, A. C.; Vaughan, D. In *X-ray Data Booklet Compiled and Edited by Lawrence Berkeley National Laboratory*, 2nd ed.; Lawrence Berkeley National Laboratory, University of California—Berkeley: Berkeley, CA, 2001.
(42) Apen, E.; Hitchcock, A. P.; Gland, J. L. *J. Phys. Chem.* **1993**, *97*, 6859−6855.
(43) Thompson, D.; Coleman, S.; Diamond, D.; Byrne, R. *Phys. Chem. Chem. Phys.* **2011**, *13*, 6156−6168.
(44) Fumino, K.; Wulf, A.; Ludwig, R. *Angew. Chem., Int. Ed.* **2008**, *47*, 8731−8734.
(45) Mori, R. A.; Paris, E.; Giuli, G.; Eeckhout, S. G.; Kavcic, M.; Zitnik, M.; Bucar, K.; Pettersson, L. G. M.; Glatzel, P. *Anal. Chem.* **2009**, *81*, 6516−6525.
(46) Fujii, K.; Fujimori, T.; Takamuku, T.; Kanzaki, R.; Umebayashi, Y.; Ishiguro, S.-I. *J. Phys. Chem. B* **2006**, *110*, 8179−8183.
(47) Umebayashi, Y.; Mitsugi, T.; Fukuda, S.; Fujimori, T.; Fujii, K.; Kanzaki, R.; Takeuchi, M.; Ishiguro, S-I *J. Phys. Chem. B* **2007**, *111*, 13028−13032.
(48) Herstedt, M.; Smirnov, M.; Johansson, P.; Chami, M.; Grondin, J.; Servant, L.; Lassègues, J. C. *J. Raman Spectrosc.* **2005**, *36*, 762−770.